Reaction fronts formation during oxygen chemical diffusion in oxides

M. Sinder *, Z. Burshtein, J. Pelleg

Materials Engineering Department, Ben-Gurion University of the Negev, P.O. Box 653, Beer-Sheva 84105, Israel

A B S T R A C T

We present a theoretical study of the impact of oxygen diffusion in oxide crystals on the dynamic changes of metal dopants in the ionic state, and on the crystal conduction type. The analysis invokes ambipolar diffusion for all participating species: oxygen vacancies, metal dopant, holes and electrons. The species dynamics are demonstrated for an oxide of 8 eV energy gap, electron and hole diffusivities being 10^5 times larger than the oxygen vacancy one, and the dopant energy level being 1.0 eV above or 1.0 eV below the mid-gap. We obtain linkage between the oxygen chemical diffusivity and the occurrence of a reaction front. The necessary condition is the existence of a sufficiently long interval, where a power dependence of the oxygen chemical diffusivity on the ambient oxygen pressure exists. In our demonstrated system, prominent reaction fronts occur at very low and at very high ambient oxygen pressures. The fronts relate to the reversible $M_{Me}^\times + e' \xleftrightarrow{} M_{Me}'$ reaction at the low pressures, and to the reversible $M_{Me}' + h^\cdot \xleftrightarrow{} M_{Me}^\times$ reaction at high pressures, where M marks the dopant metal, and Me marks an oxide lattice constituent metal. In the mid-pressure interval, the oxygen chemical diffusivity is approximately constant, being several orders of magnitude smaller than the oxygen vacancy diffusivity.

© 2015 Elsevier B.V. All rights reserved.

1. Introduction

Oxide crystals are commonly used as hosts for different metal ions, serving various optical applications such as laser gain, and light saturable absorption [1–3]. Oxygen diffusion in oxide crystals is also of interest in relation to color centers [2], as well as to valence transformations of embedded metal ions [3]. Recently, a theoretical study of the impact of oxygen diffusion in oxide crystals on the metal dopants ionic state, and on the conduction type under dynamic changes was published [4]. In that work oxygen vacancy formation acting as a shallow, double-electronic donor, was assumed to be the result of the crystal exposure to a low ambient oxygen pressure. Critical transitions from an n- to a p-type at an oxygen partial pressure P_i, and transitions in the metal dopant between two ionization states at an oxygen partial pressure P_M, are usually not simultaneous, and depend on the different reaction constants. Invoking ambipolar diffusion for all participating species, it was shown that oxygen vacancy chemical diffusion exhibits well defined characteristics in specific regions of the vacancy concentration related to the said critical pressures. Particularly, the oxygen chemical diffusivity was practically constant between P_i and P_M, and increased sharply for pressures $P \ll P_i, P_M$ and $P \gg P_i, P_M$. Seeger's analytical solution of the diffusion equations [5] was utilized for the $P \gg P_i, P_M$ regions. A step function approximation of the oxygen chemical diffusivity was applied for the $P \ll P_i, P_M$ regions.

In this communication we provide an essential improvement relative to the published article, namely, we extend the utilization of

Seeger's analytical solution to include the $P \ll P_i, P_M$ regions. It is shown, that prominent reaction fronts occur under specific conditions in the $P \ll P_i, P_M$ regions, similar to those occurring in the $P \gg P_i, P_M$ regions. In the model framework, the necessary condition for the reaction front occurrence is the existence of a sufficiently long interval which exhibits a power dependence of the oxygen chemical diffusivity on the partial oxygen pressure.

2. Model

In this communication we consider only one of the three types of the oxygen vacancies analyzed in [4,6], specifically $V_O^{\cdot\cdot}$. The oxygen vacancies involved are assumed to be shallow, each contributing two electrons to the lattice conduction band. Surface evaporation is described by the reaction

$$O_O^\times \leftrightarrow \tfrac{1}{2} O_2(\text{gas}) + V_O^{\cdot\cdot} + 2e', \tag{1}$$

where $O_O^\times$ is a lattice oxygen atom, e' is a free electron, and $V_O^{\cdot\cdot}$ is a doubly ionized oxygen vacancy. The free electron–hole reaction is given by

$$e' + h^\cdot \leftrightarrow 0, \tag{2}$$

where $h^\cdot$ is a free hole. It is assumed that the metallic dopant ion $M_{Me}^\times$ is a deep acceptor; namely, it may capture a single free electron and change into an M_{Me}' ion:

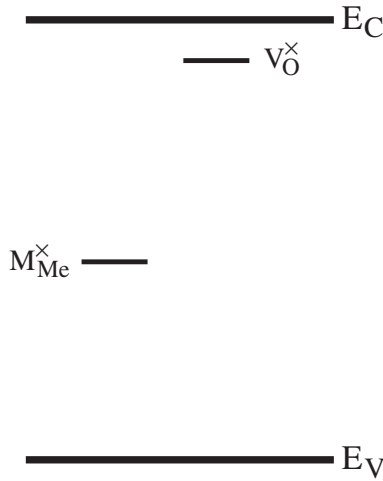$$M_{Me}^\times + e' \leftrightarrow M_{Me}'. \tag{3}$$

Fig. 1. Energy scheme for an oxide crystal, a deep $M_{Me}^{\times}$-dopant, and a shallow oxygen vacancy $V_O^{\times}$ considered in our analysis. E_V and E_C are the top valence and bottom conduction band energies, respectively.

The equilibrium reaction constants of the (1), (2), (3) reactions are denoted by K_1, K_2, and K_3, respectively, as in [6].

Fig. 1 illustrates the energy level scheme of the model.

Table 1 taken from [6] presents the energy schemes, reaction parameters and characteristic pressures used for the demonstrations in the present communication.

3. Analysis

When the crystal is subjected to a change in the ambient oxygen pressure, oxygen vacancy diffusion is activated, inducing concentration changes of the other species (metal ions, free electrons, free holes) until a new equilibrium is established. In a manner similar to [4] we consider the dynamics of these changes. Under local electro-neutrality and quasi-equilibrium of all chemical reactions, the oxygen chemical diffusivity D^{δ} should be used in the diffusion equations. Following Maier [7,8],

$$D^{\delta} = \frac{1}{\dfrac{1}{4[V_O^{\bullet\bullet}]D_V} + \dfrac{1}{[e']D_e + [h^{\bullet}]D_h}} \times \left[\frac{1}{4[V_O^{\bullet\bullet}]} + \frac{1}{(1+R_e)[e'] + [h^{\bullet}]} \right] , \quad (4)$$

where D_V, D_e, and D_h are the diffusion coefficients of the free vacancies, free electrons, and free holes, respectively, and $R_e \equiv [M]K_3/(K_3 + [e'])^2$ is the differential trapping ratio. One usually assumes that D_e, $D_h \gg D_V$. The chemical diffusion equation is then [8]

$$\frac{\partial V(x,t)}{\partial t} = \frac{\partial}{\partial x}\left[D^{\delta}(V(x,t)) \frac{\partial V(x,t)}{\partial x} \right], \quad (5)$$

Table 2
Approximate oxygen chemical diffusivity and reaction equilibrium states for different partial ambient oxygen pressure regions based on Eq. (4) above when $P_i \ll P_M$ ($\sqrt{K_2} \gg K_3$).

P	$P \ll P_i$ [a]	$P_i \ll P \ll P_M$	$P_M \ll P$ [b]
D^{δ}	$D_e \frac{K_3[M]}{([M]-2V)^2}$ $= \frac{2D_e K_1 [O_O^{\times}][M]}{K_3} \cdot P^{-1/2}$	$D_h \frac{K_2}{[M]K_3}$	$D_h \frac{3}{8} \frac{K_2[M]}{K_3 V^2}$ $= \frac{3D_h K_2 K_3^{1/3}}{2^{5/3} K_1^{2/3} [O_O^{\times}]^{2/3}[M]^{1/3}} P^{1/3}$
Reaction equilibrium state	$M_{Me}^{\times} + e' \xrightarrow{\longleftarrow} M_{Me}'$	$M_{Me}^{\times} \xrightarrow{\longleftarrow} M_{Me}' + h^{\bullet}$	$M_{Me}^{\times} \xleftarrow{\longleftarrow} M_{Me}' + h^{\bullet}$

[a] Provided $P \gg 4[O_O^{\times}]^2 K_1^2/K_3^2[M]^4$; $(D_e/D_V)^4 [O_O^{\times}]^2 K_1^2/4[M]^6$.
[b] Provided $P \ll 32(D_V/D_h)^3 [M][O_O^{\times}]^2 K_1^2/(K_2^3 K_3)$.

where for brevity $V \equiv [V_O^{\bullet}]$. Once Eq. (5) is solved, the other species concentrations are obtained using equilibrium expressions (Appendix A of Ref. [6]).

Tables 2 and 3 summarize the approximate expressions for D^{δ} when $\sqrt{K_2} \gg K_3$ and when $K_3 \gg \sqrt{K_2}$, respectively, for different regions of the ambient partial oxygen pressure. Also specified are the reaction equilibrium states for each region. The oxygen chemical diffusivity is constant between P_i and P_M; beyond this region it always depends on the pressure P, hence on the vacancy concentration V.

Next we discuss the concentration and reaction rate profiles of various species during diffusion for the $P \ll P_i$ and $P \ll P_M$ regions defined in Tables 2 and 3 under oxidation or reduction. We limit the considerations to a semi-infinite sample. In both low-pressure regions, most dopant metal ions exist in the M_{Me}' state, and the reaction equilibrium state is identical: $M_{Me}^{\times} + e' \xrightarrow{\longleftarrow} M_{Me}'$. The effective diffusivities are described by the same expression, displaying an $([M] - 2V)^{-2}$ dependence on the vacancy concentration. We denote the surface concentration of $M_{Me}^{\times}$ ions as $[M_{Me}^{\times}]_S$. Then, the oxygen chemical diffusivity is

$$D^{\delta} = D_e \frac{K_3[M]}{([M]-2V)^2} = \frac{\overline{D}}{\left([M_{Me}^{\times}]/[M_{Me}^{\times}]_S \right)^2}, \quad (6)$$

where $\overline{D} = D_e K_3[M]/\left([M_{Me}^{\times}]_S\right)^2$.

We invoke Seeger's parametric solution [5]: One defines a constant A as the solution of the equation

$$1 - A\sqrt{\pi}\,\mathbf{exp}\left(A^2\right)\mathbf{erfc}(A) = \frac{[M_{Me}^{\times}]_S}{[M_{Me}^{\times}]_0}, \quad (7)$$

where $[M_{Me}^{\times}]_0$ is the $M_{Me}^{\times}$ ion concentration at $t = 0$. For a free parameter $\lambda \geq A$

$$y \equiv \frac{x}{2\sqrt{\overline{D}t}} = \left\{ \lambda - A\,\mathbf{exp}\left(A^2 - \lambda^2\right) - \lambda A\pi^{1/2}\,\mathbf{exp}\left(A^2\right)[\mathbf{erfc}(A) - \mathbf{erfc}(\lambda)] \right\}, \quad (8a)$$

Table 1
Summary of energy schemes, reaction parameters, and characteristic pressures used for demonstrations. All relate to an energy gap $E_g = 8$ eV, lattice oxygen ion concentration $[O_O^{\times}] = 10^{22}$ cm^{-3}, temperature $k_B T = 0.1$ eV, and total metal ion concentration $[M] \equiv [M_{Me}^{\times}] + [M_{Me}'] = 10^{18}$ cm^{-3}. All characteristic pressures P_M relate to an actual oxygen partial pressure of 1 atm. For definition of the various parameters see [6].

$M_{Me}^{\times}$ ion energy position	Energy scheme	K_1	K_2	K_3	P_i	P_M
1 eV above mid-gap		10^{-4} atm$^{1/2}$ cm^{-6}	10^9 cm^{-6}	10^9 cm^{-3}	2×10^{26} atm	1.0 atm
1 eV below mid-gap		10^{-4} atm$^{1/2}$ cm^{-6}	10^9 cm^{-6}	1 cm^{-3}	2×10^{-19} atm	1.0 atm